Nonlinear dynamics and wavelets in discrete biomathematical models

Anna Maria Paolucci[*], Ezio Venturino[†]

[*]Facolta' di Informatica,
Libera Universita' di Bolzano,
39100 Bolzano,
Italy

[†]Dipartimento di Matematica,
Universita' di Torino,
via Carlo Alberto 10,
10123 Torino,
Italy

Corresponding author's e-mail: apaolucci@unibz.it

Abstract. A discrete ecoepidemiological model is considered. Its dynamics is studied by using wavelet decomposition.

1 INTRODUCTION

Dynamical systems such as the logistic map have an edge to chaos in their parameter spaces. On one side of this edge the dynamics is chaotic for many parameter values, on the other side of the edge it is periodic.

Chaos has been studied using signal processing techniques. Signal processing is a method of extracting information from the signal which depends both on the type of signal and the nature of information it carries. If the signal is stationary, it can be well represented in terms of basis functions which are sinusoidal. The time series is periodic and the spectrum consists of discrete lines. On the other hand irregular and chaotic time series all have a continuous part in their spectrum which indicates that Fourier analysis is not suitable. The signals or time series where there is chaos are nonlinear and Fourier analysis does not provide a good description of the location and spatial distribution of the singularities. A wavelet analysis provides good localization properties in frequency spaces.

In the next Section we give a brief overview of multiresolution analysis and its connection with an operator theoretic aspect as the one of representations on Hilbert spaces. This brings new insight into the study of logistic maps, attractors and operator relations in Hilbert spaces.

A discrete model for interacting species, one of which is subject to a disease, is then proposed in Section 3 and its equilibria are theoretically analyzed in Section 4. A preliminary investigation by means of simulations is then carried out, in Section 5. By means of wavelet decomposition analysis, we show that at least for the equilibrium corresponding to the single population model, it has a similar behavior than the one exhibited by the logistic map, in view also of its resemblance to it.

2 MATHEMATICAL BACKGROUND

A number of wavelet constructions in pure and applied mathematics have a common operator-theoretic underpinning, a Hilbert space H, a unitary operator $U : H \longrightarrow H$ and a unitary representation $V : \mathbf{T} \longrightarrow U(H)$ from the torus $\mathbf{T}$ into unitary operators on H.

The operator system satisfies the identity

$$V(z)^{-1}UV(z) = zU, \quad z \in U. \tag{1}$$

2

U is homogeneous of degree one if it satisfies (1) for some representation $V(z)$ of $\mathbf{T}$. In the case of standard wavelets with scale N, $H = L^2(\mathbf{R})$, the two operators U and $\mathbf{T}$ are the $N-$adic scaling and the integral translation operators respectively.

If $V_0 \subset H$ is a resolution subspace then $V_0 \subset U^{-1}V_0$. Set $W_0 = U^{-1}V_0 - V_0$. Let Q_0 denote the projection onto W_0 and let $Q_k = U^{-k}Q_0U^k$, for $k \in \mathbf{Z}$. Then $V(z) = \sum_{k=-\infty}^{+\infty} z^k Q_k$, for $k \in \mathbf{T}$. Thus $(U, V(z))$ satisfy (1).

Let $\{\Psi_i\}_{i\in I}$ be a Parseval frame in W_0. It follows that

$$\{U^k T_n \Psi_i : v \in I, k, n \in \mathbf{Z}\} \tag{2}$$

is a Parseval frame for H.

Turning the picture around, if we start with $(U, V(z))$ satisfying (1), then we reconstruct wavelet (or frame) bases in the form (2). In particular a construction of a multiresolution/wavelet analysis for the set X where the dynamics is generated by a function $r : X \longrightarrow X$. Such analysis could be accomplished by some kind of wavelet representation induced by a normal operator T such that $UT = r(T)U$ for some unitary operator U in a Hilbert space H.

There are consequences and applications of such construction. One of them is the existence of some special generating functions m_i on the set X. The required relation is

$$\frac{1}{N} \sum_{y\in X(r),\ \ r(y)=x} \overline{m_i(y)}m_j(y)h(y) = \delta(i,j)h(x)$$

almost everywhere, with $x \in X(r)$, h is a Perron-Frobenius eigenfunction for a Ruelle operator R on $L^\infty(X(r))$ and for every set X there exists an infinite-dimensional group which acts transitively on these systems of functions.

The functions m_i on $X(r)$ satisfying quadratic equations analogous to those of the axioms that define systems of filters in wavelet analysis. In further investigations we could consider Julia sets where $X = Julia(r)$, which are examples of chaotic attractors for iterative discrete dynamical systems, in the framework of the ecoepidemiological models presented in the next Sections.

3   THE ECOEPIDEMIOLOGICAL MODEL

Continuous ecoepidemiological models have been recently proposed and analyzed, see for instance [6], [7]. Here we consider an interacting population

3

system given by two species, a predator y and a prey, in which the latter is affected by a disease spreading by contact between an infectious individual z and a sound one x, with incidence rate λ. Both subpopulations are subject to predation, at the same rate c, but we assume that the disease does not spread to the predator's population. Furthermore, let A denote the environment's prey carrying capacity.

Only the sound prey is assumed to reproduce, giving sound newborns, with net birth rate r. The population pressure for the sound prey gives rise to a logistic term, to which also the infected individuals contribute. We also assume that the disease is recoverable, i.e. infected become once again susceptibles at rate γ. The disease induces a mortality rate μ for infected individuals.

The predators in absence of prey are assumed to die at an exponential rate d, i.e. the prey constitute their only source of food, they being turned into new predators with efficiency e.

We assume that the populations are counted at fixed time intervals, between which successive generations are born and die out, thus giving rise to a discrete dynamical system. With these assumptions thus, the model equations read as follows.

$$x_{n+1} = rx_n[1 - \frac{1}{A}(x_n + z_n)] - \lambda x_n z_n - cx_n y_n + \gamma z_n \qquad (3)$$
$$z_{n+1} = \lambda x_n z_n - cz_n y_n - \gamma z_n - \mu z_n$$
$$y_{n+1} = y_n[-d + e(x_n + z_n)]$$

4   EQUILIBRIA DETERMINATION

The equilibria are the origin $O \equiv E^{(0)}$ and the points $E^{(i)} = (x^{(i)}, z^{(i)}, y^{(i)})$, $i = 1, \ldots, 4$ where

$$E^{(1)} \equiv (\frac{1+d}{e}, 0, \frac{eA(r-1) - r(1+d)}{ceA}),$$

$$E^{(2)} \equiv (\frac{r-1}{r}A, 0, 0),$$

$$E^{(3)} \equiv (\frac{1+\gamma+\mu}{\lambda}, \frac{1+\gamma+\mu}{\lambda} \quad \frac{\lambda A(1-r) + r(1+\gamma+\mu)}{r\gamma + (1+\mu)(\lambda A + r)}, 0),$$

4

$$E^{(4)} \equiv \left(\frac{d\gamma A}{d(r + \lambda A) - eA(r + \mu)}, \frac{d}{e} - x^{(4)}, \frac{1}{c}(\lambda x^{(4)} - 1 - \gamma - \mu)\right).$$

The Jacobian of the dynamical system at these equilibria is easily found:

$$\tilde{J} = \begin{pmatrix} r - \frac{2r}{A}\tilde{x} - [\lambda + \frac{r}{A}]\tilde{z} - c\tilde{y} & -\frac{r}{A}\tilde{x} - \lambda\tilde{x} + \gamma & -c\tilde{x} \\ \lambda\tilde{z} & \lambda\tilde{x} - c\tilde{y} - \gamma - \mu & -c\tilde{z} \\ e\tilde{y} & e\tilde{y} & e(\tilde{x} + \tilde{z}) - d \end{pmatrix}$$

where $\tilde{J} = J(\tilde{E})$ and $\tilde{E} = (\tilde{x}, \tilde{z}, \tilde{y})$ denotes either one of the five equilibria $E^{(i)}$, $i = 0, 4$.

The eigenvalues $\eta_j^{(i)}$, $j = 1, 2, 3$, $i = 0, \dots, 4$ at each possible equilibrium in some cases are explicitly found, as follows. Notice that the stability condition requires that $|\eta_j| \le 1$ for each $j = 1, 2, 3$.

At the origin, they are r, $-\gamma - \mu$ and $-d$. At $E^{(1)}$ they are $\lambda x^{(1)} - cy^{(1)} - \gamma - \mu$, and the roots of the quadratic equation

$$u^2 - u[r + 1 - 2\frac{r}{A}x^{(1)} - cy^{(1)}] + [r - 2\frac{r}{A}x^{(1)} - cy^{(1)}] + cex^{(1)}y^{(1)} = 0.$$

At the point $E^{(2)}$ we find instead $ex^{(2)} - d = eA(1 - \frac{1}{r}) - d$, $\lambda A(1 - \frac{1}{r}) - \gamma - \mu$, $-r$. At $E^{(3)}$ they are $e(x^{(3)} + z^{(3)}) - d$ and the roots of the quadratic

$$u^2 - b_1 u + b_0 = 0$$

with

$$b_1 \equiv 1 + r(1 - \frac{1}{A}(x^{(3)} + z^{(3)})) - \lambda z^{(3)} - \frac{r}{A}x^{(3)}$$

and

$$b_0 \equiv r(1 - \frac{1}{A}(x^{(3)} + z^{(3)})) - \lambda z^{(3)} - \frac{r}{A}x^{(3)} + \lambda z^{(3)}[(\frac{r}{A} + \lambda)x^{(3)} + \gamma] = 0.$$

Finally the interior equilibrium $E^{(4)}$ has eigenvalues coming from the solution of a complete cubic equation.

5   SYSTEM DYNAMICS ANALYSIS

For comparison sake, we recall the classical analysis performed on the single species logistic equation

$$s_{n+1} = rs_n \left(1 - \frac{s_n}{A}\right) \equiv f(s_n). \tag{4}$$

For the nontrivial equilibrium $s^* = \frac{A}{r}(r-1)$, it is well known that the stability condition reduces to having the birth rate satisfy the inequalities $1 < r < 3$. For larger values, period doubling for the map f arises. Thus two new fixed points for f^2 are found, compare the two pictures in Figure 1. The stability of these new equilibria holds for $r > 3$ and lying in an interval of length smaller than 2, say $r \in [3, r^{(1)}]$. Then for $r > r^{(1)}$, new fixed points can be found for f^4, their stability being confined to $r \in [r^{(1)}, r^{(2)}]$, with interval length still smaller than the former one. The process can be iterated, finding new equilibria with stability intervals of diminishing length, until ultimately a value r^* is reached after which, i.e. for $r > r^*$, chaotic behavior arises. In [1] this behavior has been captured by decomposing the simulations using wavelet filters. Some of our own simulations along these lines for some selected values of r are reported in Figures 1-9.

We have attempted the use of the same technique on the proposed ecoepidemiological model (3), focusing on the corresponding equilibrium counterpart of s^*, the disease and predator-free point $E^{(2)}$. In Figures 10-18 the simulations and corresponding signal decomposition about $E^{(2)}$ are reported. From these results, it seems that the same chaotic behavior arises in both cases. A careful comparison of Figures 2 and 11 for instance, shows only small differences. Notice indeed that the vertical scale, automatically adjusted by the MATLAB Wavelet Toolbox package used for these computations, is different in the two cases. Figures 3 and 12 i.e. for the periodic maps, show some slight differences in the decomposition in the components d_3 and d_5. These discrepancies appear much more marked in the chaotic regime, compare Figures 5 and 14, in which all components essentially differ, while they are still present, but less relevant, in the range past the critical one, $r = 4.05$, compare Figures 6 and 15. Here a_5 and d_5 are basically the same, again pay attention to the vertical scale which is of the order of 10^3 in both cases. For $r = 5.8$ the differences are contained in the components d_2, d_3 and d_4, see Figures 9 and 18. This apparently occurs in spite of the presence of the other model equilibria, which are clearly absent in the one-dimensional formulation (4). While the dynamics in the one dimensional case is pushed away from s^*, in a sense wandering around, in principle in the ecoepidemic model the other equilibria could function as further stable attractors, thus preventing the occurrence of the chaotic behavior of the system trajectories from the destabilized equilibrium $E^{(2)}$. We have shown that this is not the case, though. It should also be remarked that some other preliminary simulations do not show similar chaotic phenomena to arise near the other equilibria of

6

the ecoepidemic model. Further investigation is needed.

6 CONCLUSIONS

Certain special representations of the Cuntz algebras in Hilbert spaces serve
as a tool in generating orthonormal bases in the context of wavelets and more
generally for iterated function systems, [4], [5]. Since the representations of
the Cuntz algebras naturally yield bases with n-fold scaling, from further
investigations we expect different and new operator relations arising from
the problem at hand in view of the wavelet multiresolution algebra used to
detect chaos in logistic maps.

References

[1] S. Azad, S.K. Sett, Wavelets detecting chaos in logistic map, National
Conference on Nonlinear Systems & Dynamics, NCNSD-2005, p. 301-
304.

[2] M. Baym, A.W. Hübler, Conserved quantities and adapting to the edge
of chaos in self-adjusting dynamical systems with wavelet filtered feed-
back, APS/123-QED.

[3] F. Brauer, C. Castillo-Chavez, Mathematical models in population bi-
ology and epidemiology, Springer Verlag, New York, 2001.

[4] J. Cuntz, Simple C^*-algebras generated by isometries, Comm. Math.
Phys. 57, 1977, p. 173-185.

[5] O. Bratteli, P. Jorgensen, Wavelets through a looking glass, Birkhäuser
2002.

[6] E. Venturino, Epidemics in predator-prey models: disease among the
prey, in O. Arino, D. Axelrod, M. Kimmel, M. Langlais: *Mathematical
Population Dynamics: Analysis of Heterogeneity, Vol. one: Theory of
Epidemics*, Wuertz Publishing Ltd, Winnipeg, Canada, 1995, p. 381-
393.

[7] E. Venturino, The effects of diseases on competing species, Math. Biosc.,
174, 2001, p. 111-131.
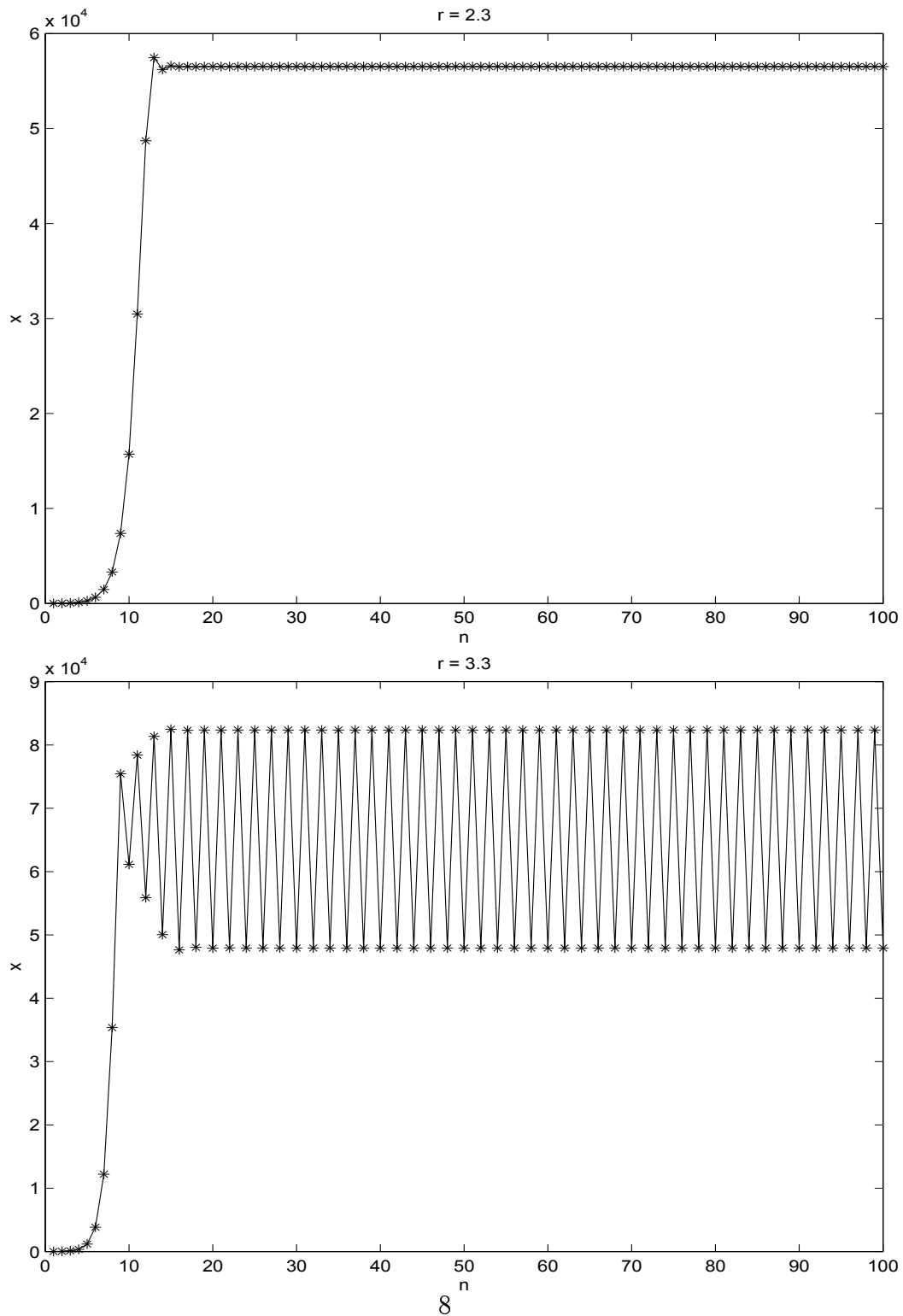
Figure 1: Simulation for the one population logistic model, $r = 2.3$ (top) and for $r = 3.3$ (bottom)

Decomposition at level 5 : s = a5 + d5 + d4 + d3 + d2 + d1 .

x 10⁴

s

a₅

d₅

d₄

d₃

d₂

d₁

Data (Size)   y (100)
Wavelet   haar
Level   5

Analyze

Statistics   Compress

Histograms   De-noise

Display mode :

Full Decomposition

at level   5

Show Synthesized Sig.
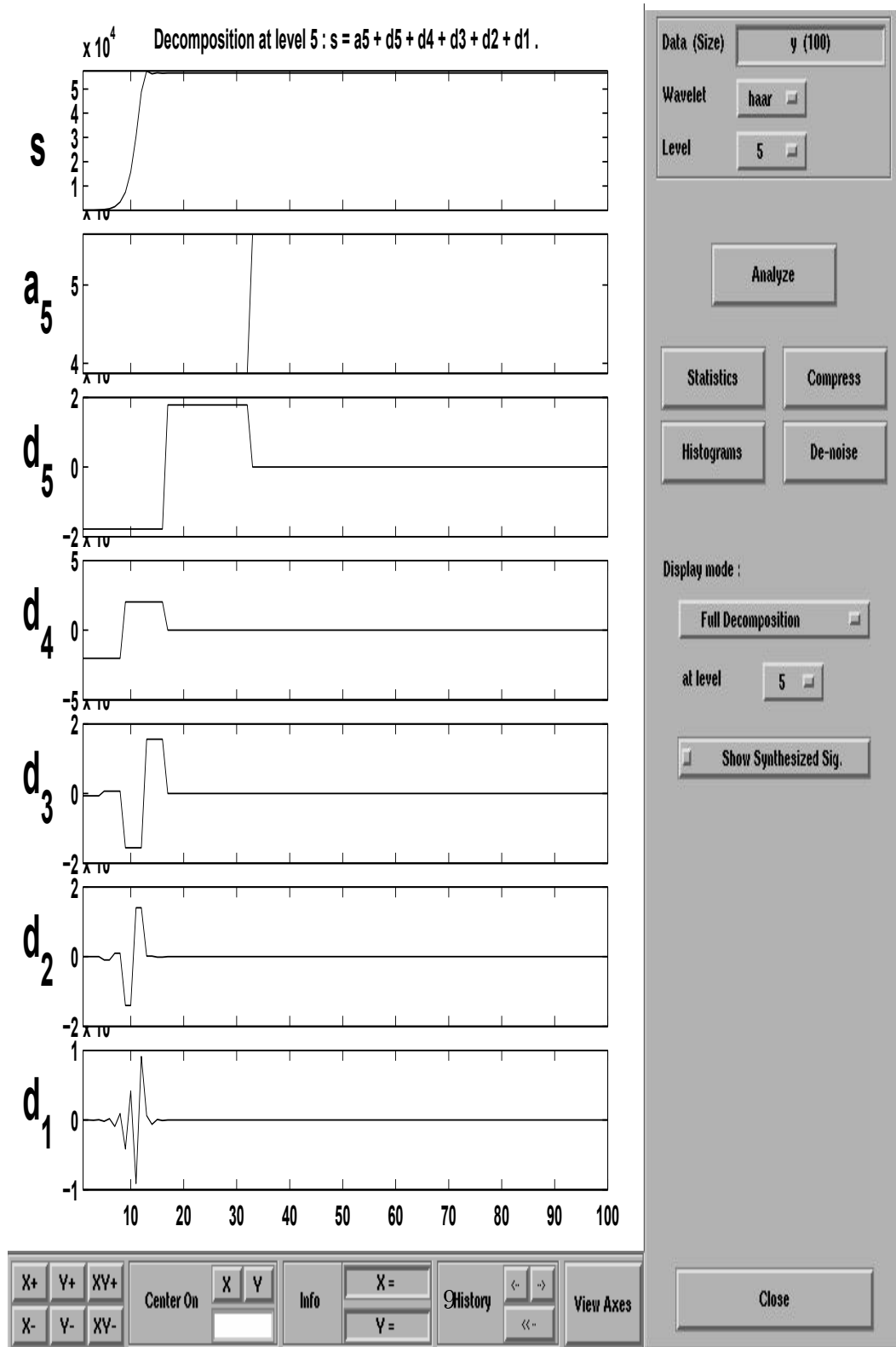
Figure 2: Analysis of the one population logistic model, $r = 2.3$
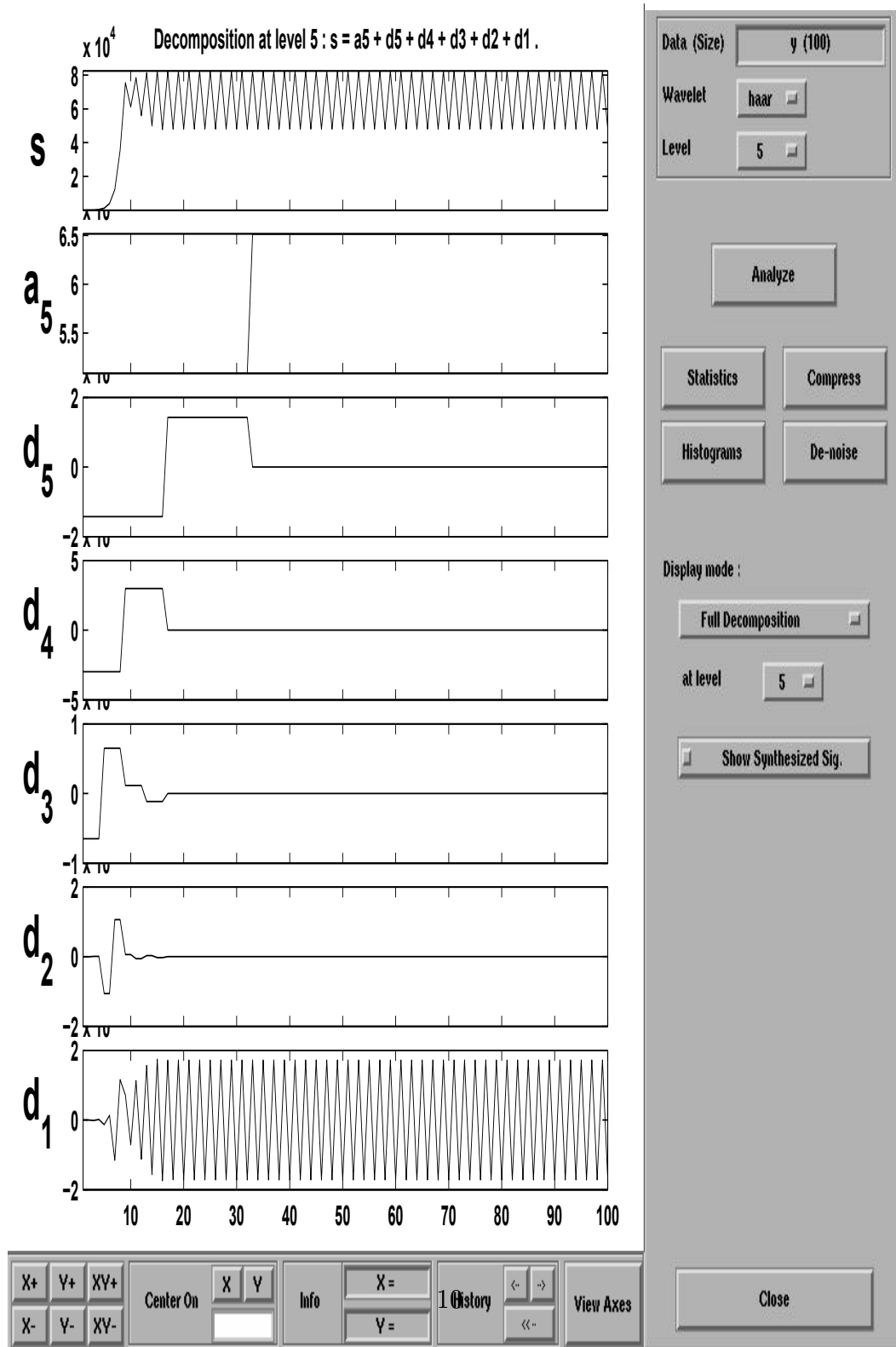
Figure 3: Analysis of the one population logistic model, $r = 3.3$
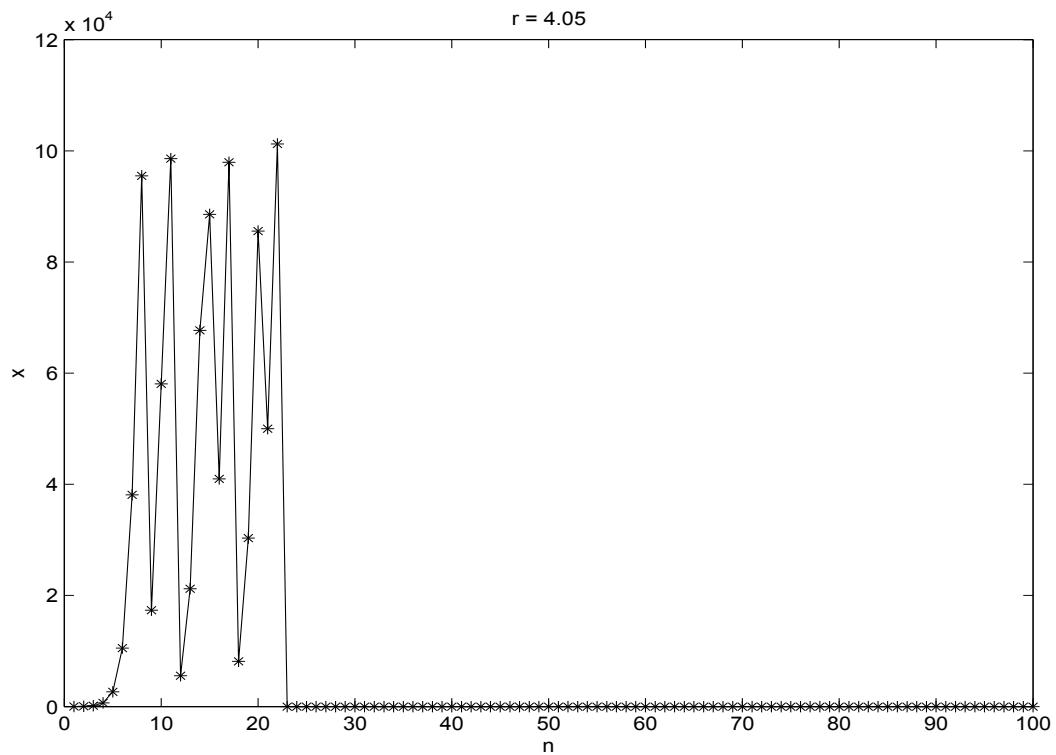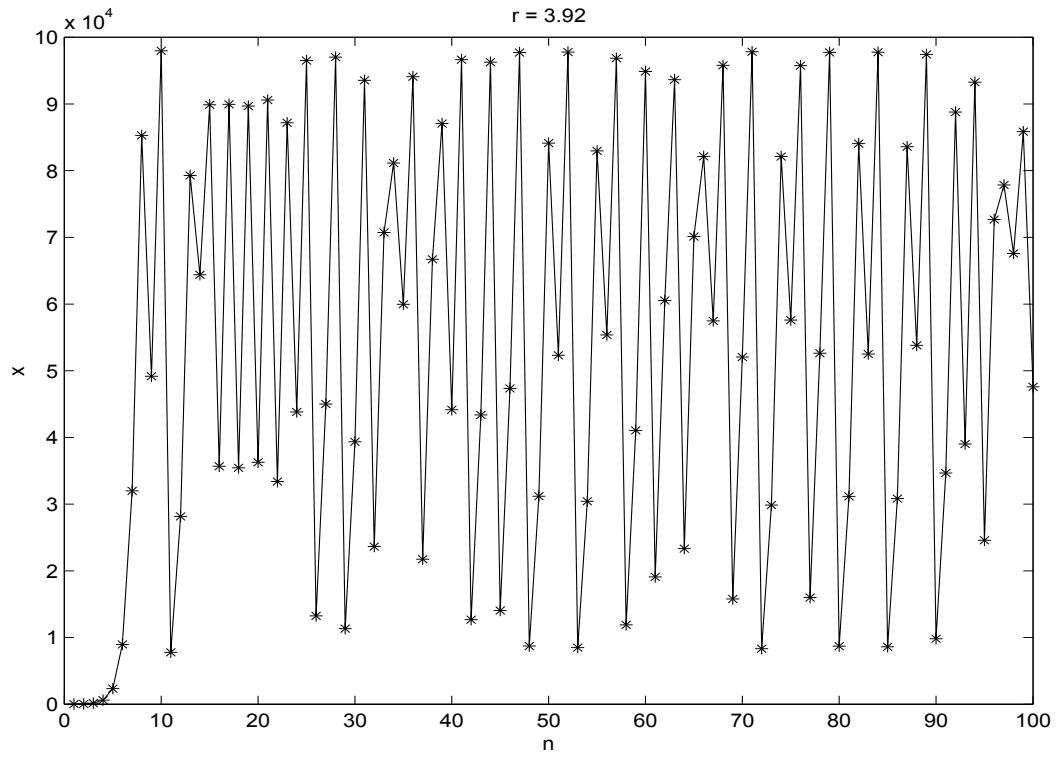
Figure 4: Simulation for the one population logistic model, $r = 3.92$ (top) and for $r = 4.05$ (bottom)

11
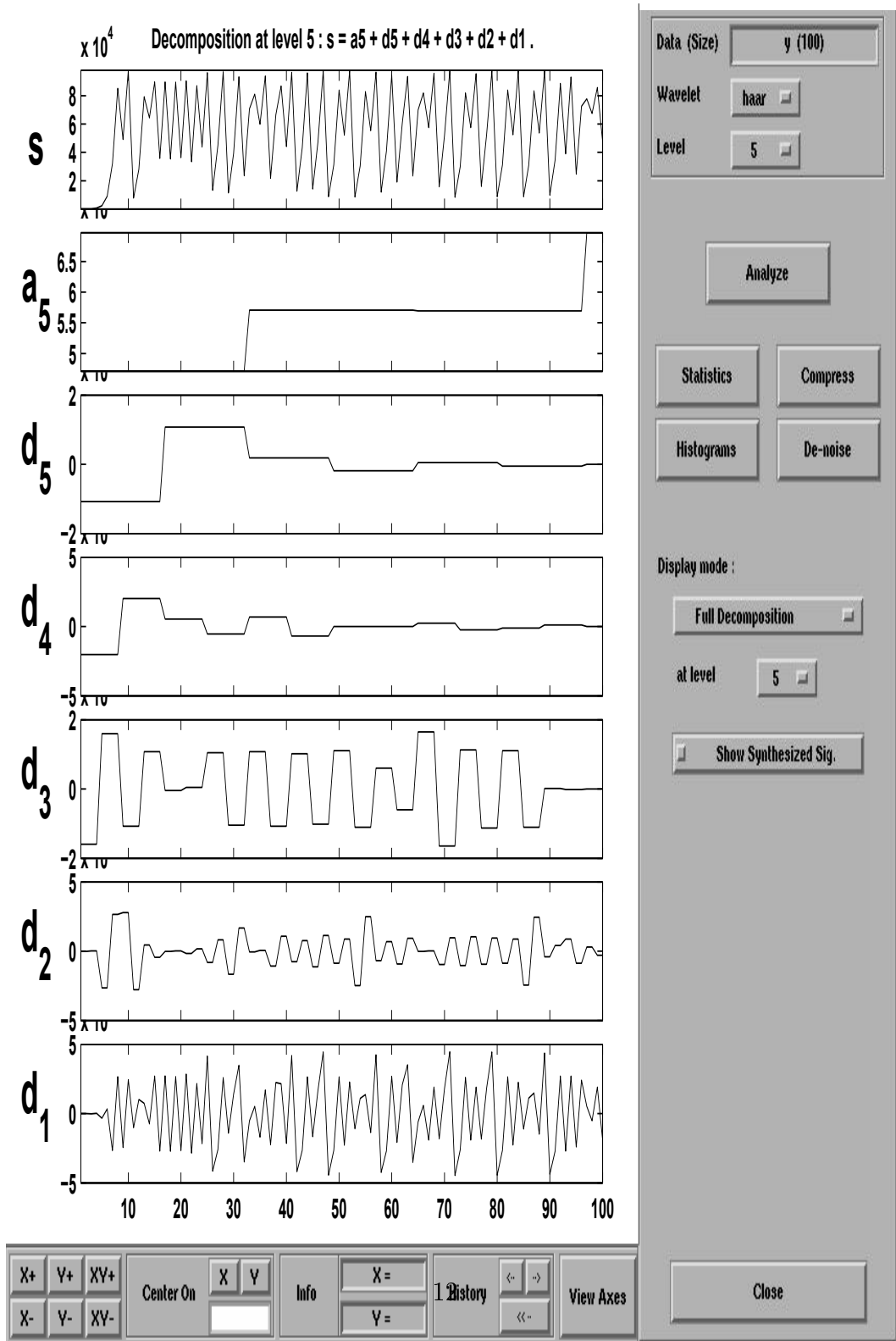
Figure 5: Analysis of the one population logistic model, $r = 3.92$
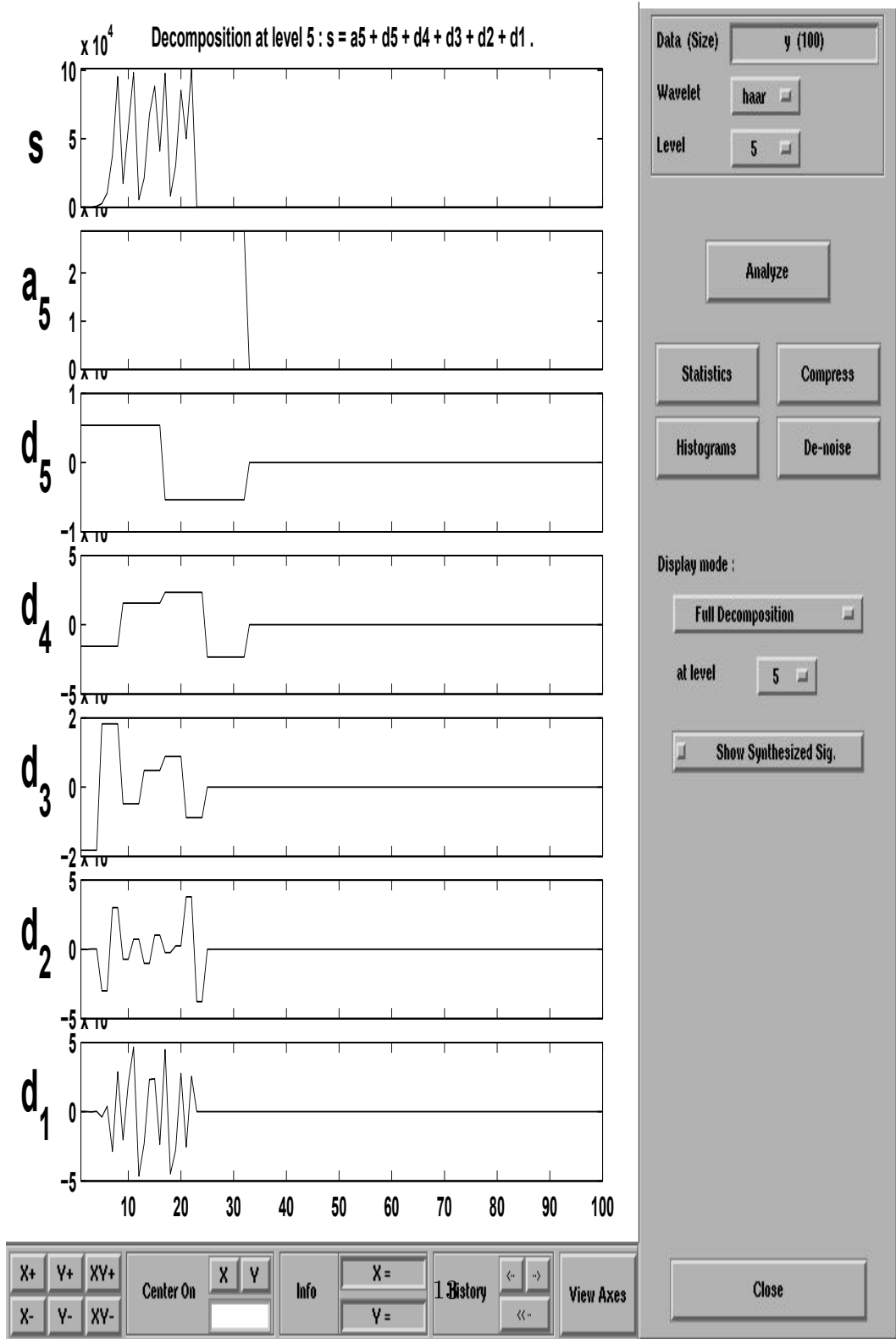
Figure 6: Analysis of the one population logistic model, $r = 4.05$
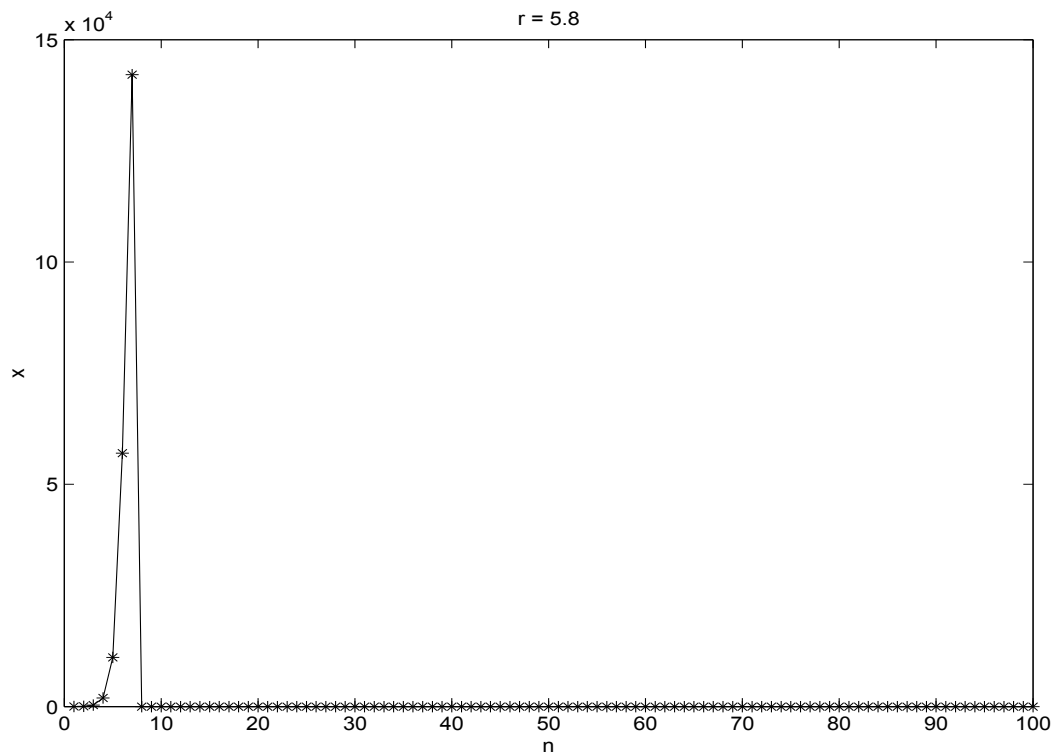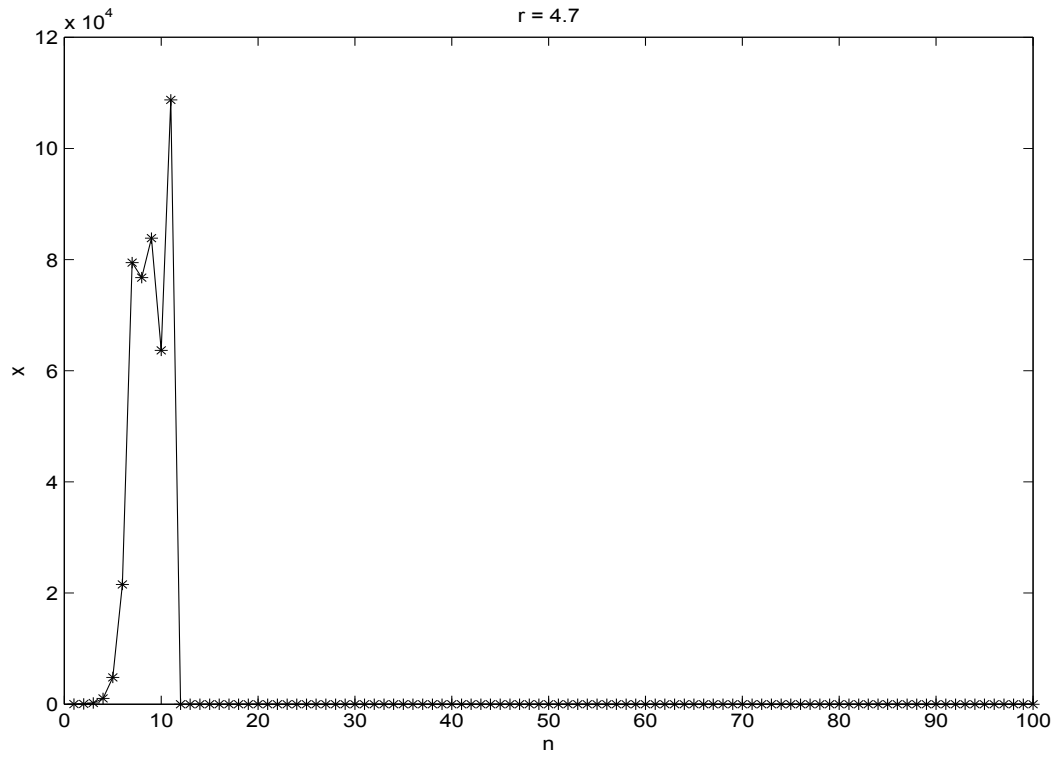
Figure 7: Simulation for the one population logistic model, $r = 4.7$ (top) and for $r = 5.8$ (bottom)

Decomposition at level 5 : s = a5 + d5 + d4 + d3 + d2 + d1 .
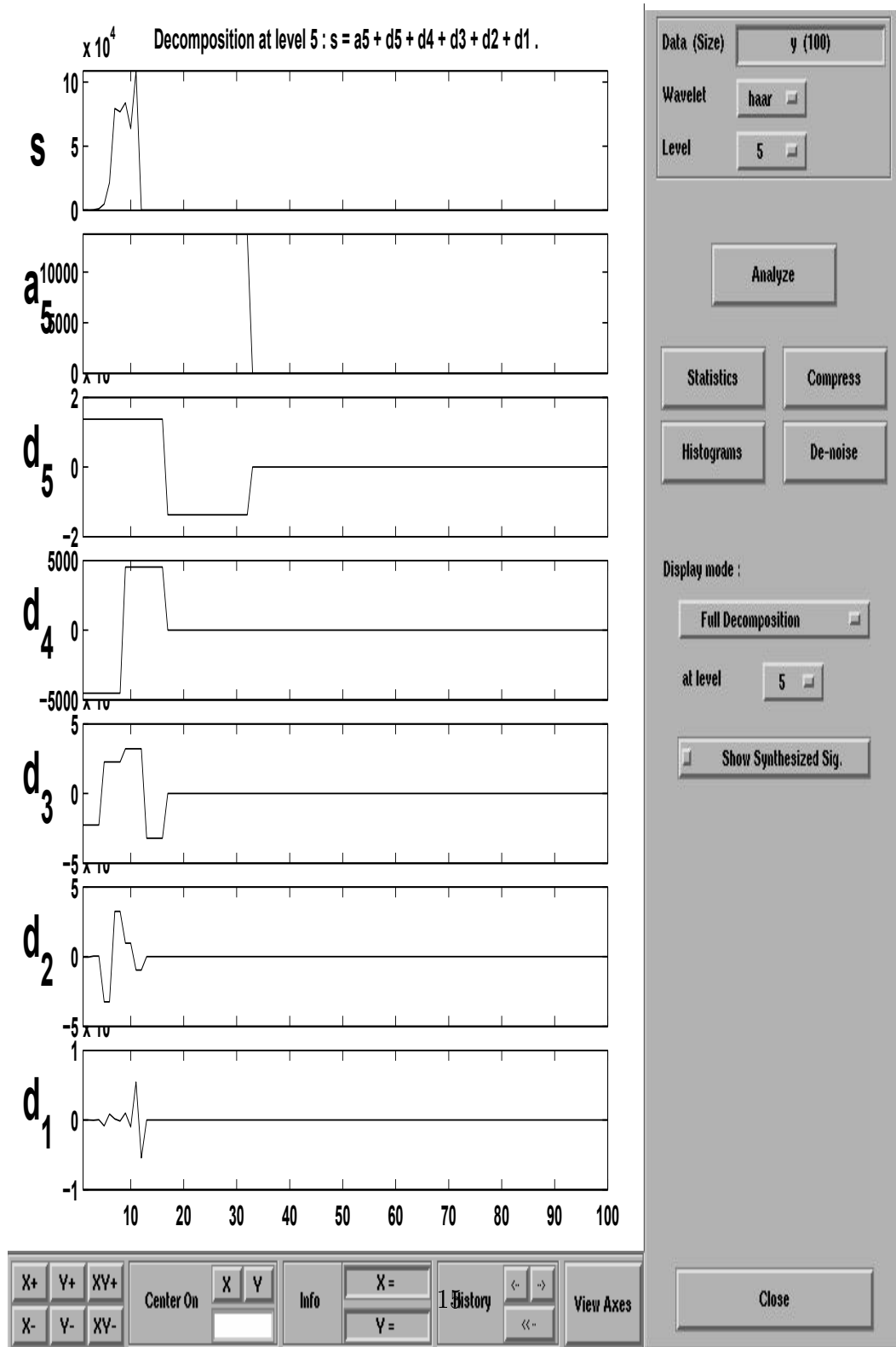
Figure 8: Analysis of the one population logistic model, $r = 4.7$
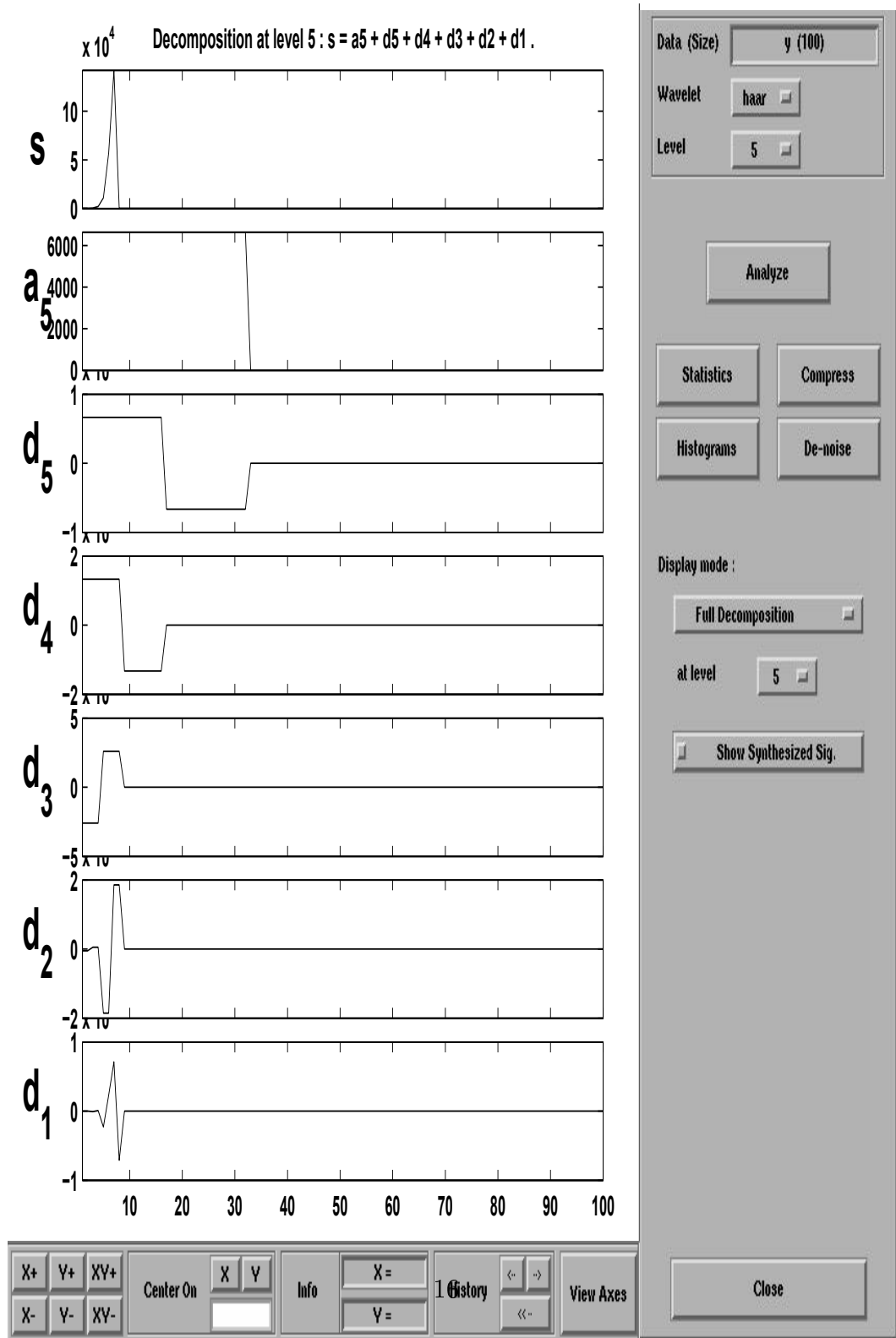
Figure 9: Analysis of the one population logistic model, $r = 5.8$
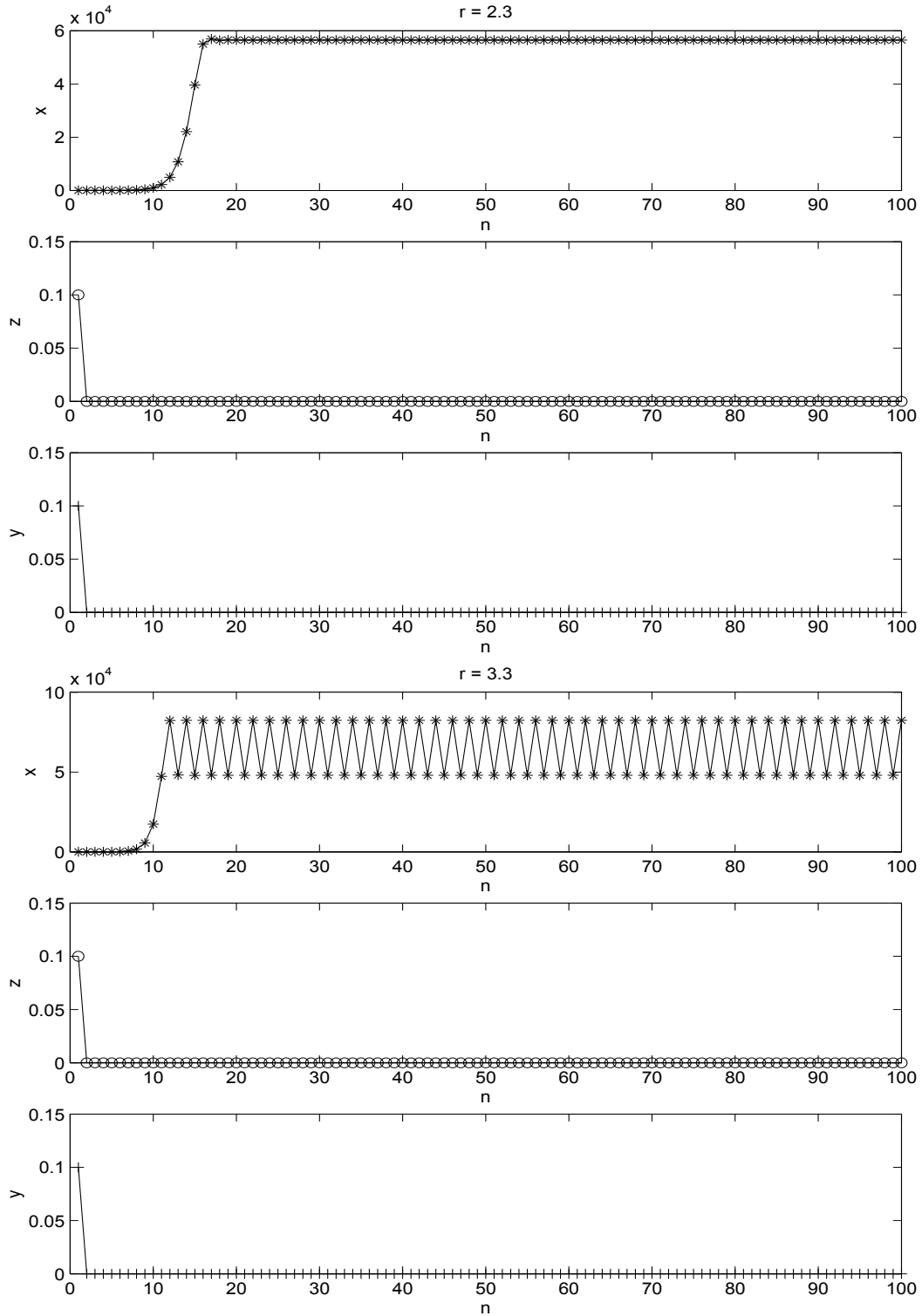
Figure 10: Simulation for the ecoepidemic model, $r = 2.3$ (top) and for $r = 3.3$ (bottom)
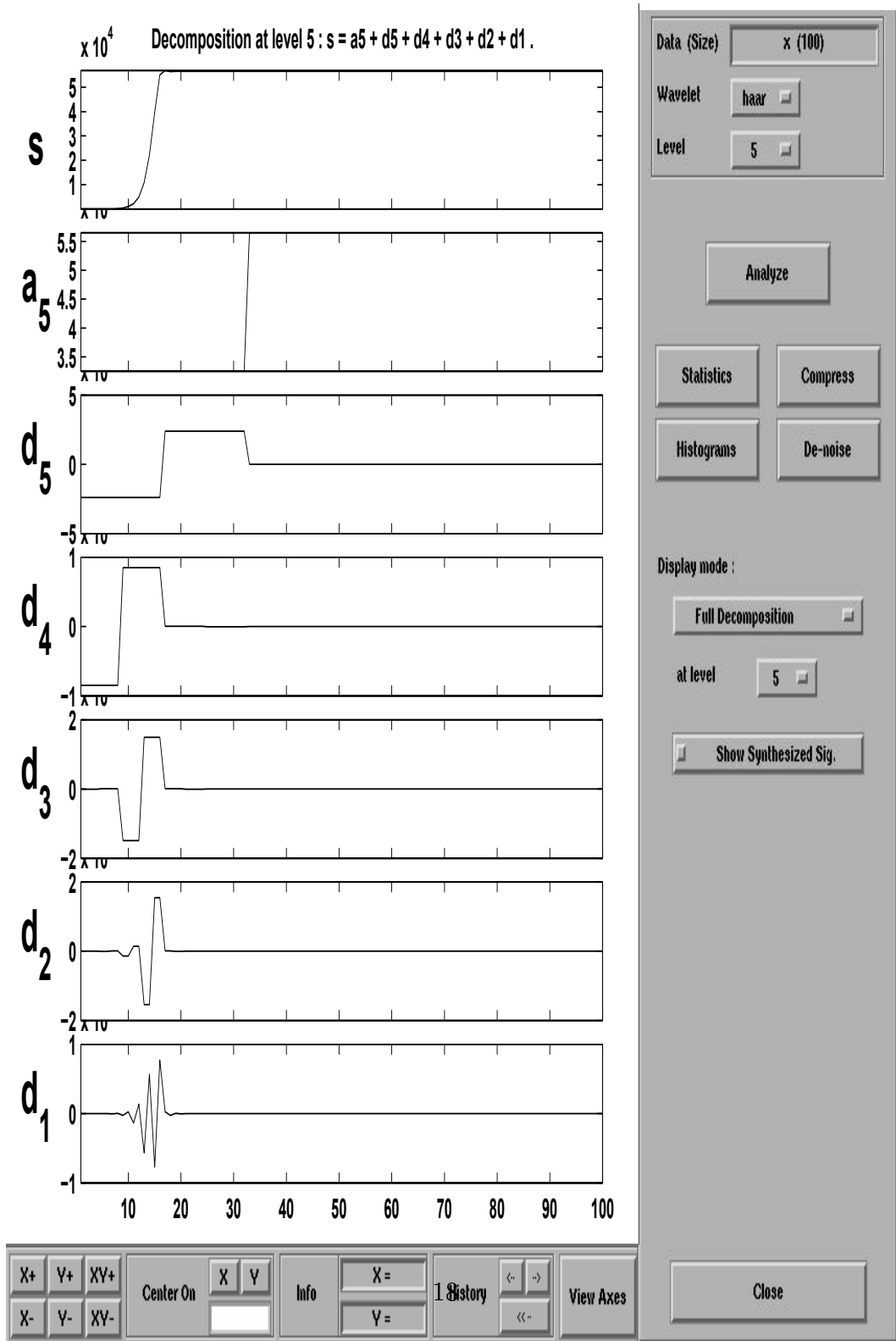
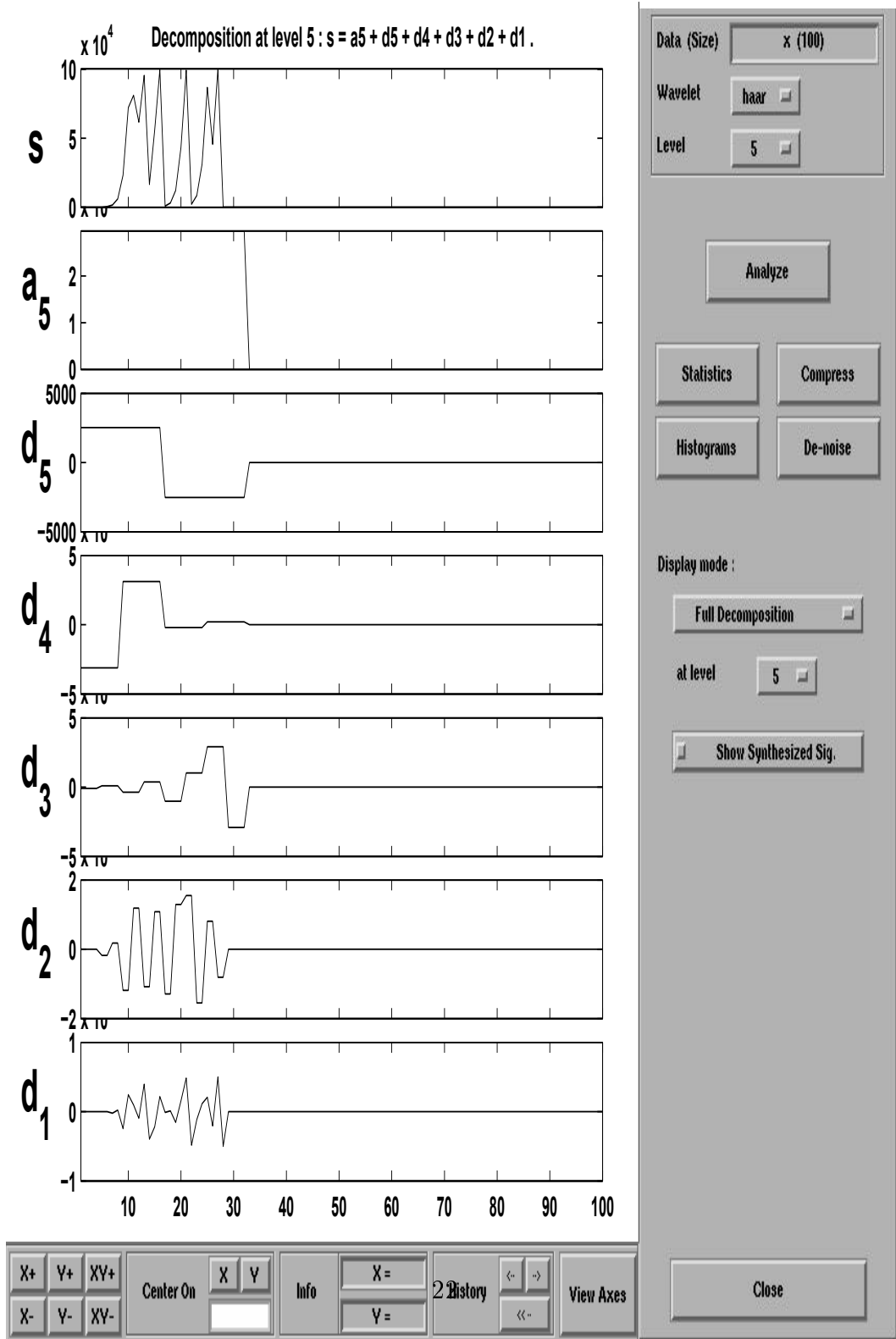Figure 11: Analysis of the sound prey in the ecoepidemic model, $r = 2.3$
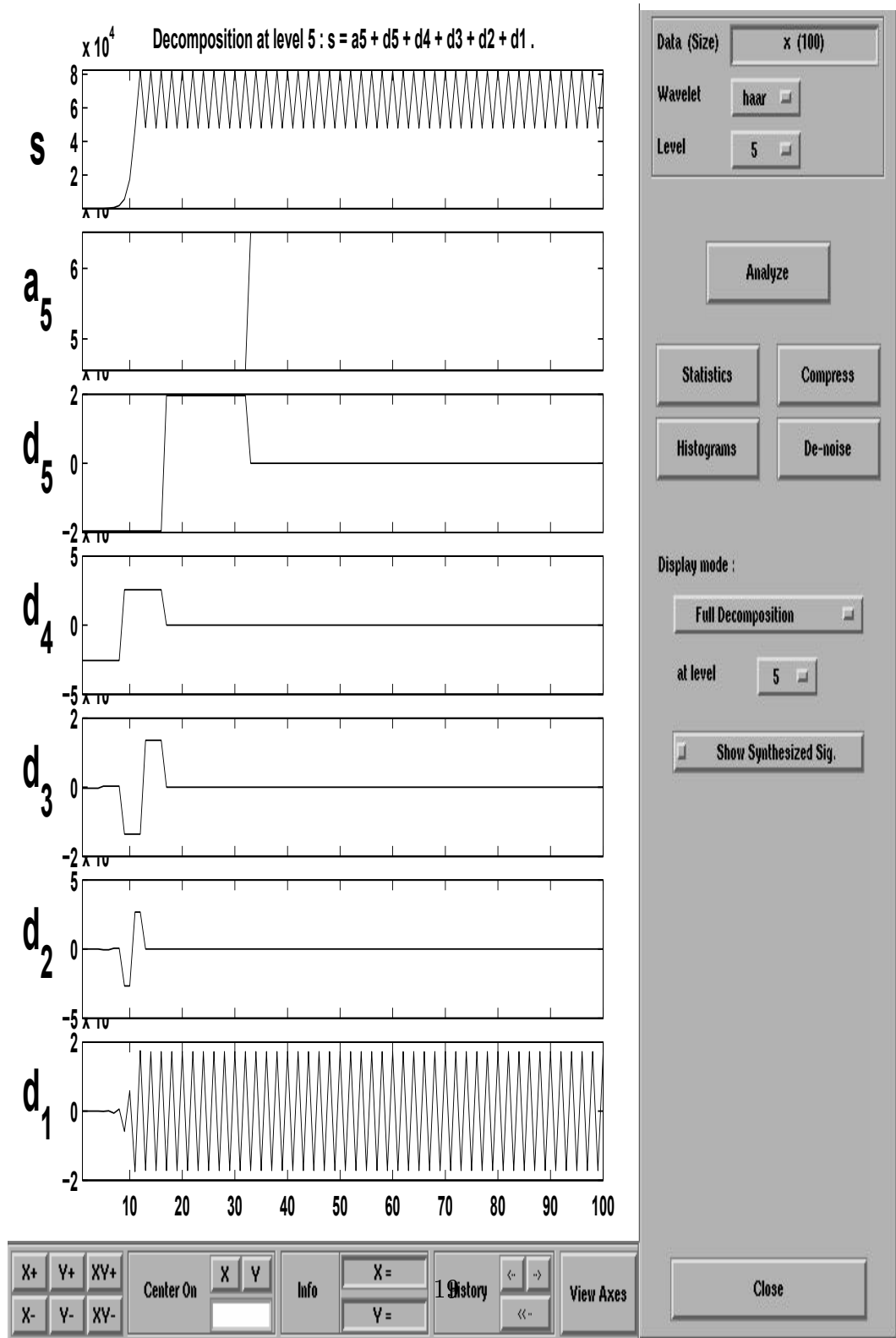
Figure 12: Analysis of the sound prey in the ecoepidemic model, $r = 3.3$
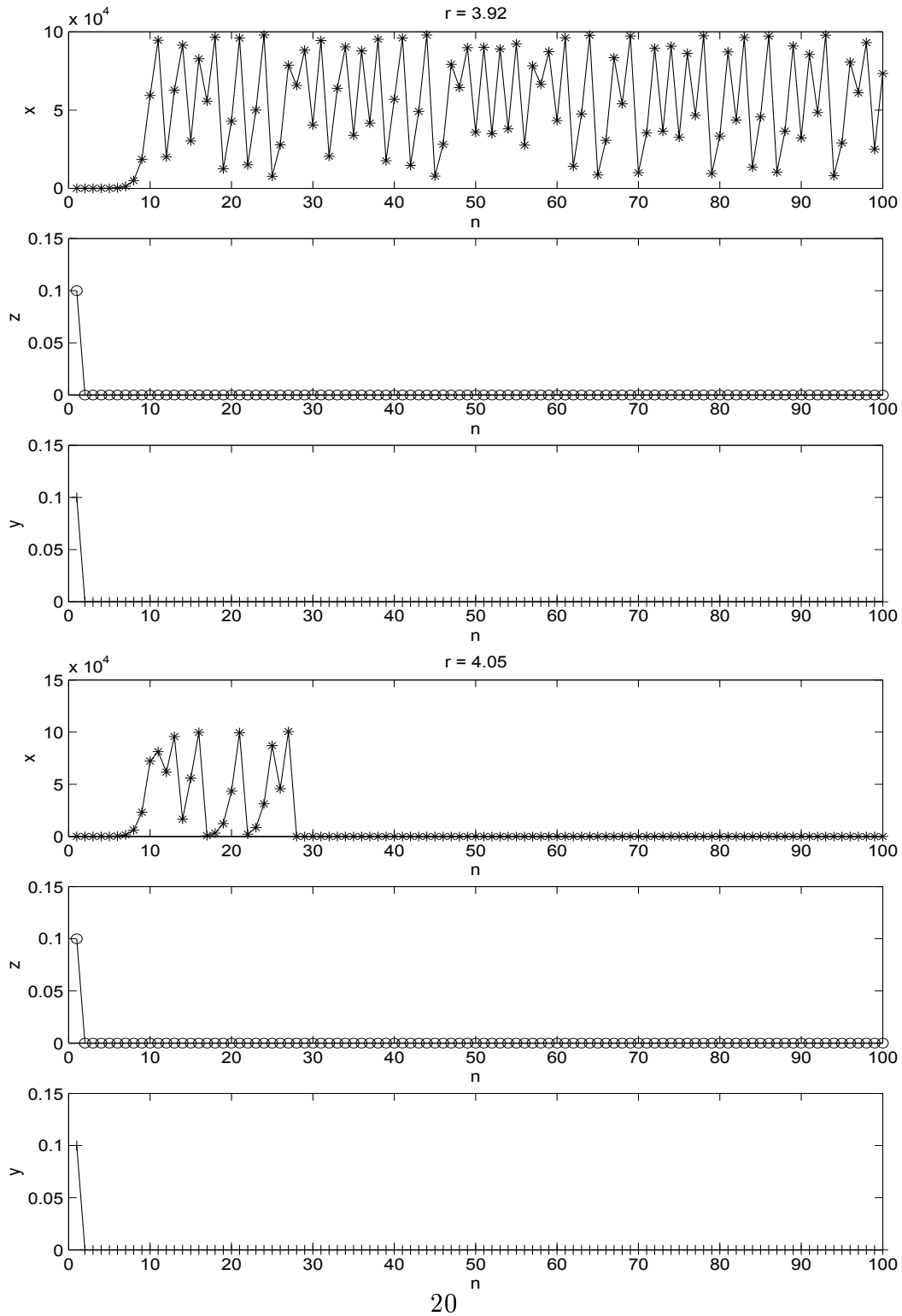
Figure 13: Simulation for the ecoepidemic model, $r = 3.92$ (top) and for $r = 4.05$ (bottom)
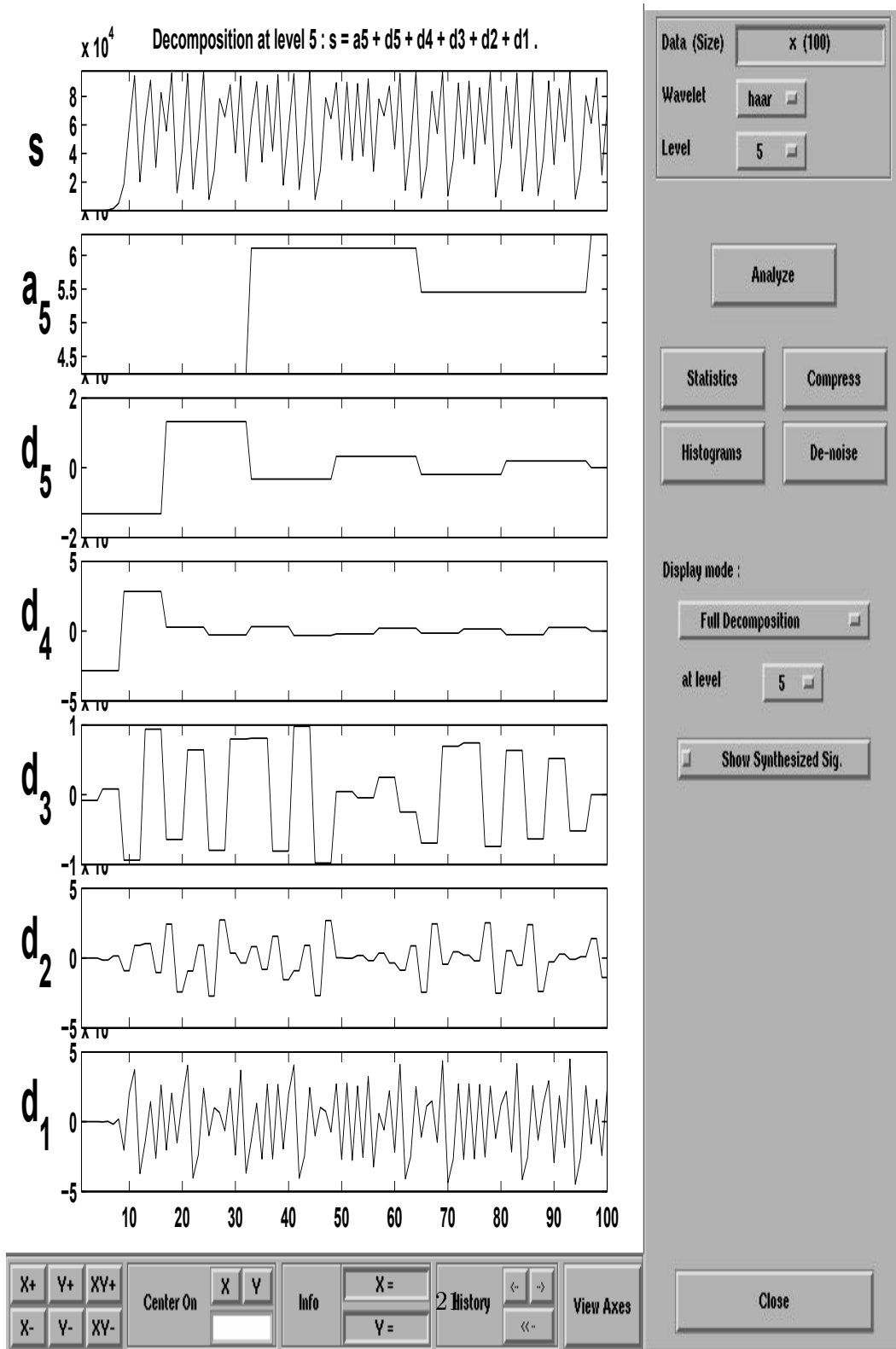
Figure 14: Analysis of the sound prey in the ecoepidemic model, $r = 3.92$

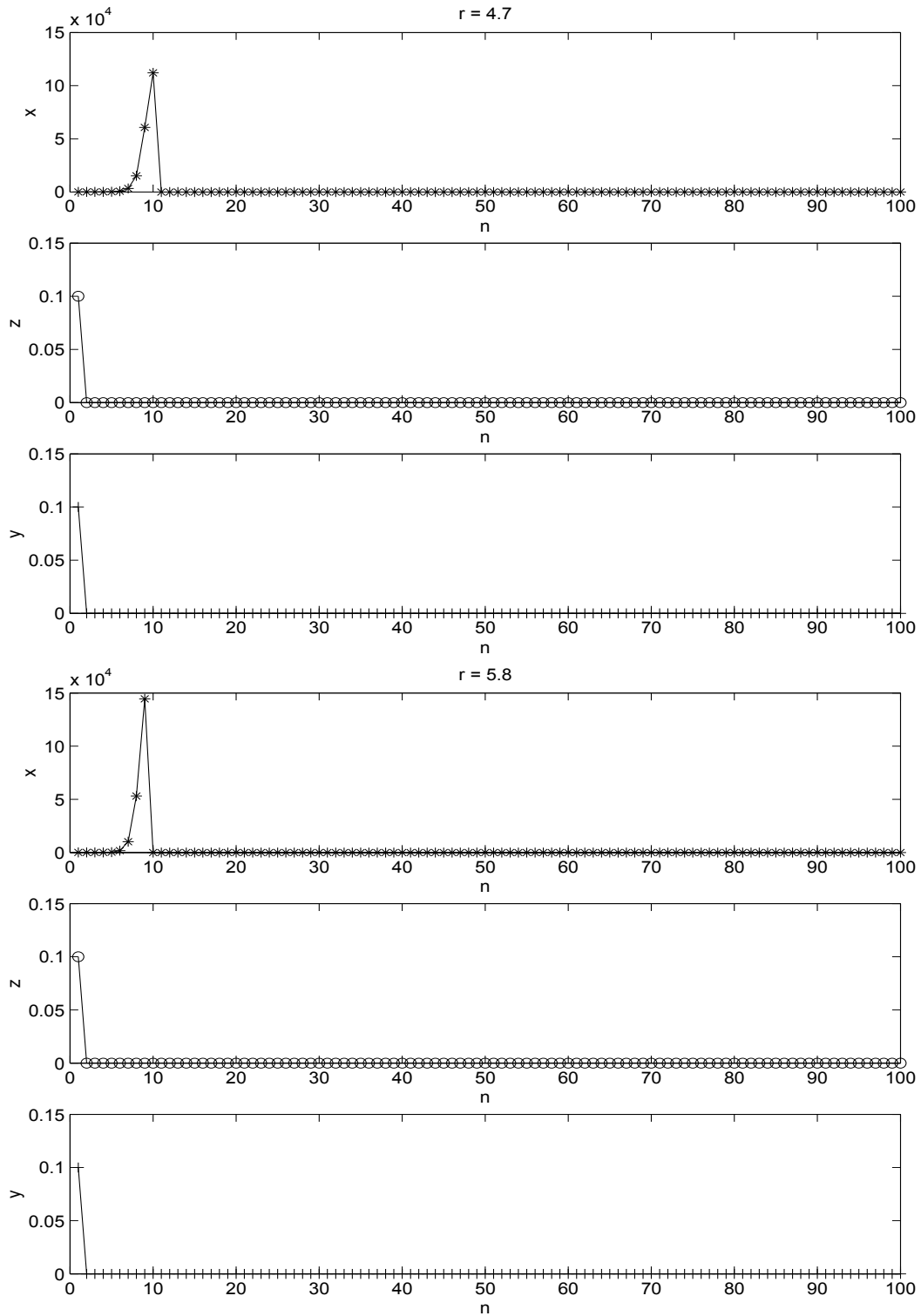Figure 15: Analysis of the sound prey in the ecoepidemic model, $r = 4.05$

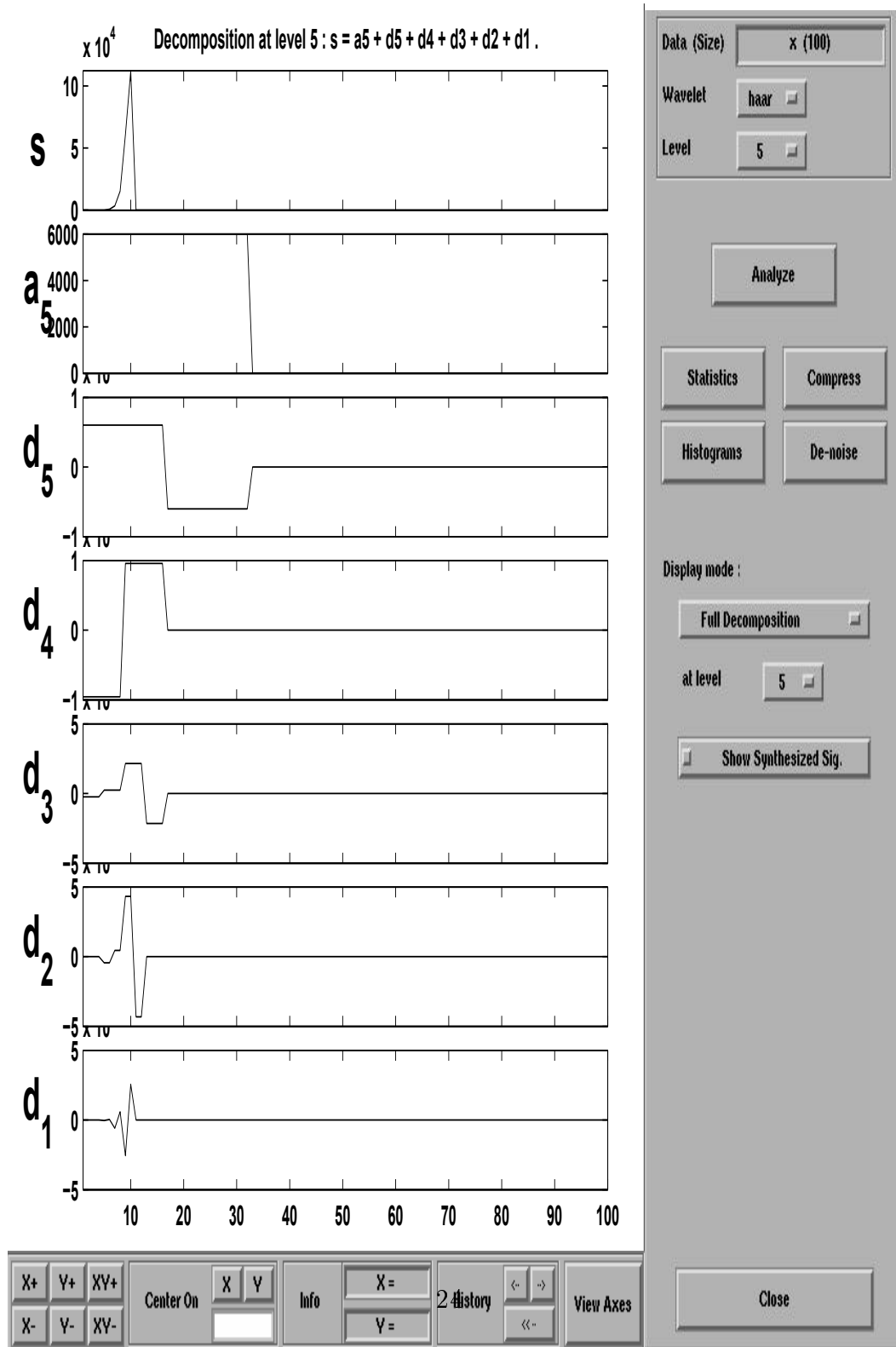Figure 16: Simulation for the ecoepidemic model, $r = 4.7$ (top) and for $r = 5.8$ (bottom)

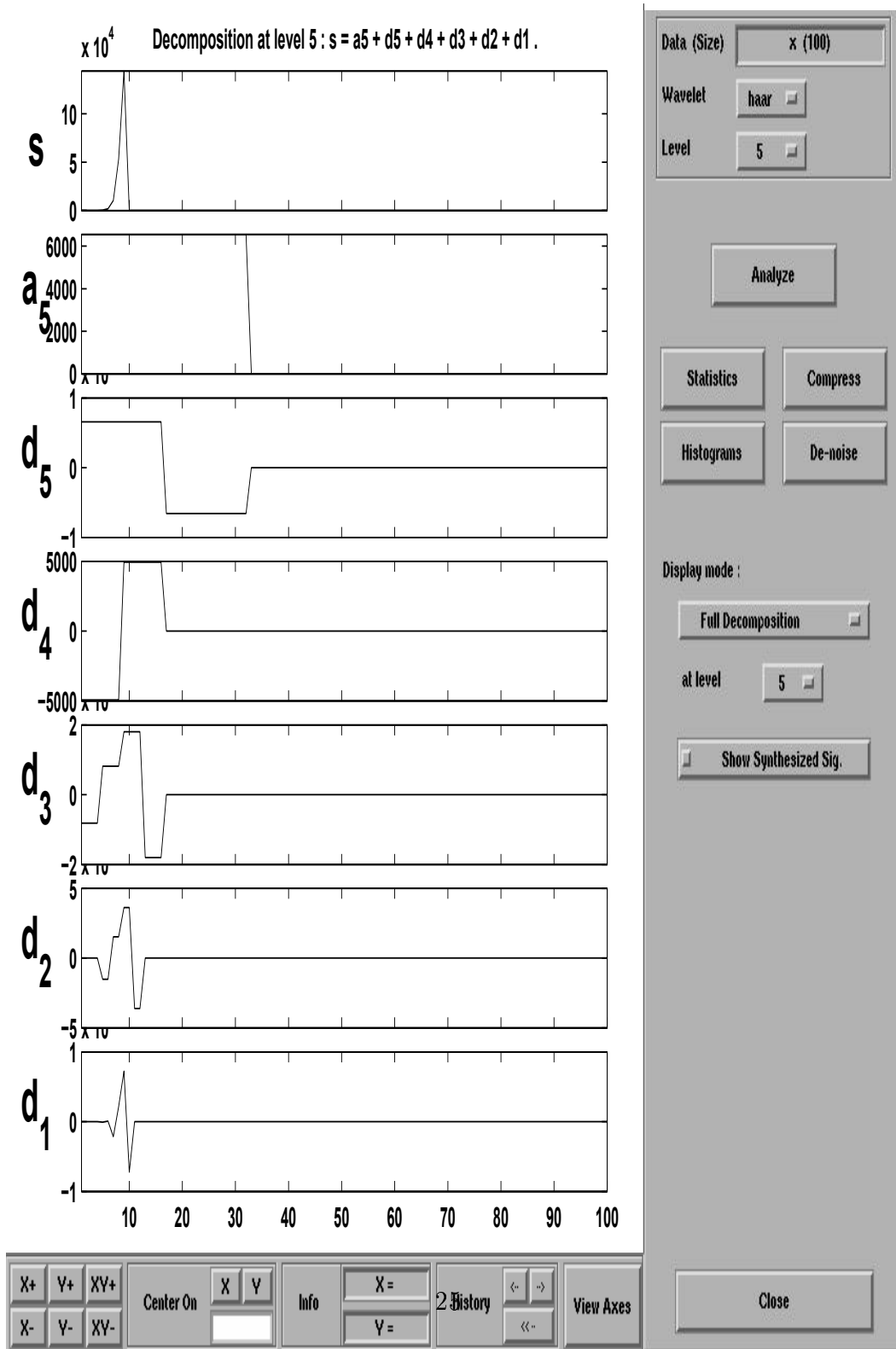Figure 17: Analysis of the sound prey in the ecoepidemic model, $r = 4.7$

Figure 18: Analysis of the sound prey in the ecoepidemic model, $r = 5.8$